TABLE OF CONTENTS

	Page	
LIST OF FIGURES	iv	1/A6
LIST OF SYMBOLS	v	1/A7
ACKNOWLEDGMENTS	viii	1/A10
CHAPTER I. INTRODUCTION	1	1/A11
CHAPTER II. AN ANALYSIS OF THE SOUNDING OF AUGUST 28, 1976	7	1/B3
CHAPTER III. GRAVITY WAVES AND RAY-TRACING THEORY	12	1/B8
CHAPTER IV. CALCULATION OF THE CONVECTIVE ENERGY INPUT	22	1/C4
CHAPTER V. THE MODEL OF GRAVITY WAVE STRUCTURE	29	1/C11
CHAPTER VI. CALCULATION OF HEATING RATES	38	1/D6
CHAPTER VII. CONCLUSIONS	48	1/E2
REFERENCES	52	1/E6

NAS1-26:3132

MAY 3 1979

NASA Contractor Report 3132

COMPLETED

ORIGINAL

Mesospheric Heating Due to Intense Tropospheric Convection

Lauren Ludlum Taylor

CONTRACT NAS6-2818
APRIL 1979

NASA

63

NASA Contractor Report 3132

Mesospheric Heating Due to Intense Tropospheric Convection

Lauren Ludlum Taylor
The Pennsylvania State University
University Park, Pennsylvania

Prepared for
Wallops Flight Center
under Contract NAS6-2818

National Aeronautics
and Space Administration

Scientific and Technical
Information Office

1979

BLANK PAGE

TABLE OF CONTENTS

	Page
LIST OF FIGURES	iv
LIST OF SYMBOLS	v
ACKNOWLEDGMENTS	viii
CHAPTER I. INTRODUCTION	1
CHAPTER II. AN ANALYSIS OF THE SOUNDING OF AUGUST 28, 1976	7
CHAPTER III. GRAVITY WAVES AND RAY-TRACING THEORY	12
CHAPTER IV. CALCULATION OF THE CONVECTIVE ENERGY INPUT	22
CHAPTER V. THE MODEL OF GRAVITY WAVE STRUCTURE	29
CHAPTER VI. CALCULATION OF HEATING RATES	38
CHAPTER VII. CONCLUSIONS	48
REFERENCES	52

LIST OF FIGURES

Figure		Page
1	Temperature as a function of height at Wallops Island, Va.	3
2	Temperature sounding at Wallops Island, Va. for 1200 Z, August 28, 1976	8
3	Raypaths of gravity wave groups initiated at 15 km on August 28, 1976.	19
4	Fate of gravity wave groups identified by dominant wavelength and periods in atmosphere of August 28, 1976.	21
5	Idealized penetrative element (a) as a function of time and (b) as a function of distance.	23
6	Spectral energy density J as a function of (a) frequency and (b) wavenumber.	24
7	Smoothed east-west wind profile for August 28, 1976 at Wallops Island, Va.	34
8	Amplitude of vertical perturbation velocity w' as a function of height.	36
9	Amplitude of horizontal perturbation velocity u' as a function of height.	37
10	Eddy viscosity coefficient K as a function of height.	39
11	Heating rates as a function of height, August 28, 1976.	42
12	Heating rates as a function of height, August 28, 1976.	43
13	Heating rates as a function of height, August 28, 1976.	44
14	Heating rates as a function of height, September 2, 1976.	45
15	Heating rates as a function of height, September 2, 1976.	46
16	Heating rates as a function of height, September 2, 1976.	47

LIST OF SYMBOLS

c	speed of sound
c_p	specific heat of air at constant pressure
c_v	specific heat of air at constant volume
d	distance parcel penetrates into stable region
f	frequency of overshooting convective element equal to $2\pi/P$
g	acceleration due to gravity
i	square root of -1
k	wavenumber in x direction
k_H	horizontal wavenumber equal to $(k^2 + \ell^2)^{1/2}$
ℓ	wavenumber in y direction
m	wavenumber in z direction
p	pressure
$\bar{p}$	mean pressure
p'	perturbation pressure
$\tilde{p}$	rescaled pressure
q	heat per unit mass
t	time
u	horizontal velocity in x direction
$\bar{u}$	mean horizontal velocity
u'	horizontal perturbation velocity
$\tilde{u}$	rescaled horizontal velocity perturbation
u_g	horizontal (east-west) group velocity
w	vertical velocity
$\bar{w}$	mean vertical velocity ($\bar{w} = 0$)
w'	vertical velocity perturbation

$\tilde{w}$	rescaled vertical velocity perturbation
w_g	vertical group velocity
x	east-west direction
y	north-south direction
z	vertical direction
D	diameter of penetrative element at equilibrium level
H	measure of scale height
J	spectral energy density function
$\overline{J}$	mean value of energy density function
K	eddy viscosity coefficient
KE	kinetic energy
N	Brunt-Väisälä frequency
P	period of overshooting convective element
$\tilde{P}$	amplitude of pressure perturbation variable $p'/\overline{\rho}$
R	universal gas constant
$\tilde{R}$	amplitude of density perturbation variable $\rho'/\overline{\rho}$
T	temperature
T_e	temperature of the environment
T_p	temperature of the parcel
U	mean or background horizontal velocity
$\tilde{U}$	amplitude of horizontal velocity perturbation u'
$\tilde{W}$	amplitude of vertical velocity perturbation w'
α	specific volume
γ	ratio of specific heats
Δk_H	horizontal wavenumber increment

Δz	height increment
$\Delta\omega_i$	Doppler-shifted frequency increment
θ	potential temperature
κ_H	parameter equal to π/D
λ_H	horizontal wavelength
π	3.14159
ρ	density
$\bar{\rho}$	mean density; reference density
ρ'	perturbation density
$\tilde{\sigma}$	rescaled buoyancy force per unit mass
ϕ	horizontal angle in wavenumber space
ω	frequency
ω_i	Doppler-shifted frequency (ω-kU)

ACKNOWLEDGEMENTS

The author wishes to thank her thesis advisor, Dr. John H. E. Clark, for introducing her to the subject matter of this research and for his continuing guidance and patience throughout its progress. The constructive criticism of the manuscript offered by Dr. John J. Olivero was also appreciated.

Financial support and rocket data has been provided by NASA-Wallops Flight Center, Virginia under NASA Grant NAS-6-2818.

CHAPTER I. INTRODUCTION

The upper atmosphere (the atmosphere above the troposphere) has long been a data-void and therefore, mysterious region. Contrary to the lower atmosphere (the troposphere), where easily available data contributed to the development of the equations, theories and models that form the basis for modern weather forecasting, knowledge of the properties of the upper atmosphere were based, until recently, on widely scattered wind and temperature measurements derived from meteor trails and from balloons penetrating the stratosphere. Now, measurements taken regularly by rockets carrying meteorological instruments have begun to supply the data which will help solve the mysteries of the upper atmosphere.

From these measurements, in a span of time little more than one decade, scientists have compiled a comprehensive climatology of the stratosphere and mesosphere. Individual soundings, however, sometimes showed large deviations from expected values. Researchers have sought to explain these deviations as products of interactions between regions of the atmosphere, particularly as consequences of the transfers of energy between the lower atmosphere (the troposphere) and the upper atmosphere. This thesis examines one such possible interaction between the lower and upper atmospheres; namely, the effect of tropospheric convection in the form of thunderstorms on temperatures observed at mesospheric heights.

From August 15 through September 10, 1976, the National Aeronautics and Space Administration (NASA) launched one or two meteorological rockets each day from Wallops Island, Va. The rockets reached altitudes ranging from 70-90 kilometers and instruments released from

these rockets measured vertical profiles of temperature, wind, density and pressure. Examination of the temperature profiles revealed that on three of the days, August 28, September 2 and September 10, a portion of the mesosphere (about 60-70 kilometers) exhibited temperatures 10-15 degrees K warmer than on preceding or following days. (See Figure 1 for plots of temperature versus height for two of the days, August 28 and September 2). Synoptic records for the three days indicate that only on these three days in the period from August 15 through September 10, intense convective activity in the form of thunderstorms and showers occurred at Wallops Island. The storms began 4-12 hours before the rocket was launched. Clearly, these occurrences make it tempting and also reasonable to try to link the thunderstorm activity with the mesospheric heating in some way.

In this study, atmospheric internal gravity waves are proposed as the coupling mechanism. Gravity waves arise when a parcel is displaced in a statically stable atmosphere (one in which the environmental lapse rate is less than the adiabatic lapse rate). The restoring force produces an oscillation of the parcel with a characteristic frequency called the Brunt-Väisälä frequency. The oscillation produces a broad spectrum of waves called gravity waves. Among other wave-like phenomena in the atmosphere, they fit between the high-frequency, short-wavelength acoustic waves and the low-frequency, long-wavelength planetary and Rossby waves. Only gravity waves with frequencies less than the Brunt-Väisälä frequency are internal gravity waves, i.e., propagate energy vertically and only these will be considered.

The excitation of gravity waves by updrafts penetrating a stable layer (common in thunderstorms), called penetrative convection, has

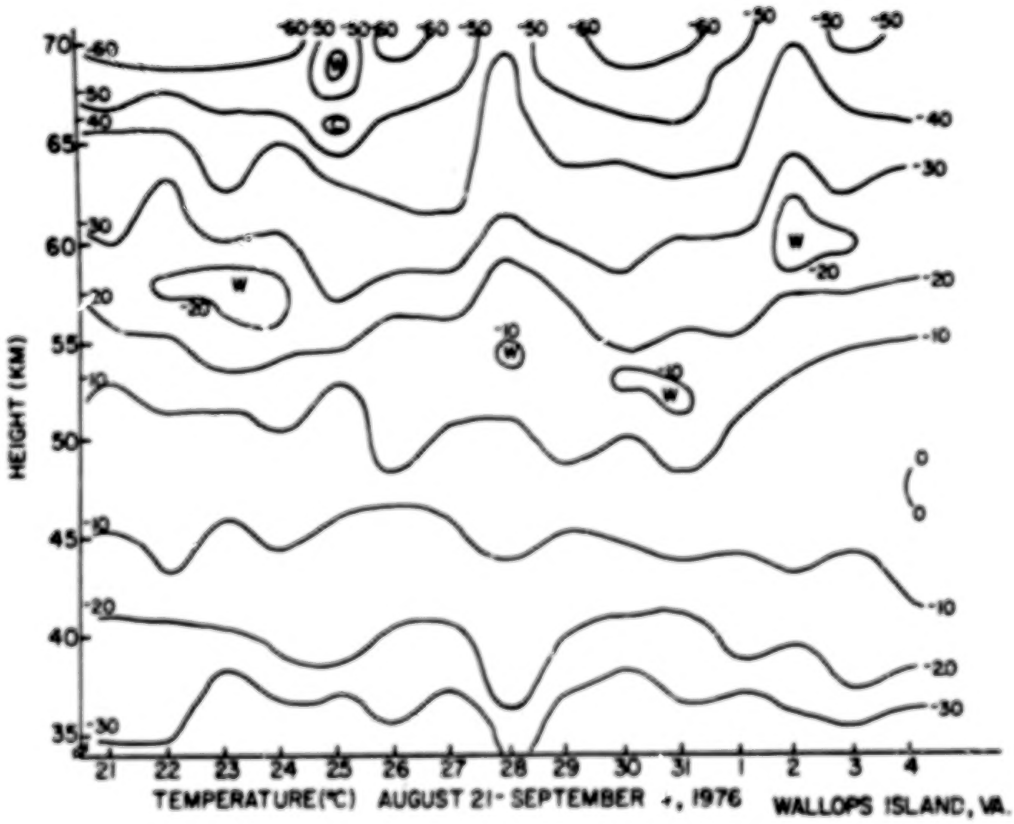

Figure 1. Temperature as a function of height at Wallops Island, Va.

been studied by many researchers (Townsend, 1965, 1966, 1968; Stull, 1976). Pierce and Coroniti (1966) considered thunderstorms specifically as a means of generating gravity waves. Therefore, the fact that thunderstorms can be considered a source for vertically propagating gravity waves is one reason for choosing them as a means of coupling the upper and lower atmospheres.

Another reason is that gravity waves have been observed at upper atmospheric heights. Many researchers (Hines, 1960, 1963, 1965; Gossard, 1962; Midgely and Liemohn, 1966; Hooke, 1968; Harris et al., 1969, to name only a few) have documented and developed theories accounting for their presence. Also, the temperature profiles for the days on which the heating occurred show a superimposed wave-like structure with vertical wavelengths ranging from 5 to 10 kilometers which is evidence of vertically propagating wave phenomena the size of gravity waves.

A third reason for suspecting that interval gravity waves excited by thunderstorms would have an effect on the mesosphere derives from the exponential decrease of atmospheric density ρ with height and the principle of the conservation of energy. In order for the wave's kinetic energy per unit volume, $\rho u'^2$, to remain constant as ρ decreases exponentially, the perturbation velocity associated with the wave, u', must increase exponentially. Therefore, waves originally generated in the troposphere will have grown considerably by the time they reach mesospheric heights and they will have sufficient magnitude to affect motions in the upper atmosphere.

As the gravity waves propagate upwards through the atmosphere, kinetic energy will be associated with the velocity perturbations

produced by them. The dissipation of this energy can heat the atmosphere. It is this heating that will be calculated and compared to the observed heating in Figure 1.

Thus, the purpose of this thesis is to account for the observed mesospheric heating through the mechanism of vertically propagating gravity waves generated by convective activity.

In Chapter II, the tropospheric sounding for one of the days of the observed heating, August 28, 1976, is analyzed to estimate the vertical velocity of a thunderstorm updraft on that day. The data for August 28 is used throughout this thesis to explain the procedures. The same procedures are used on the data of September 2, 1976, and only the results are reported. The data of September 10, 1976, was discarded since this was the last day of data collection by NASA and it is not known for certain that the temperatures returned to normal the next day.

In Chapter III, some basic theory concerning gravity wave propagation is reviewed, including ray-tracing. Ray-tracing theory assumes waves travel in packets or groups that can be identified by a dominant wavenumber and frequency. These wave groups travel at local group velocities along paths called rays. Whether the raypath of a certain wave group reaches the mesosphere depends on its dominant wavenumber and frequency as well as the temperature and wind structure of the atmosphere. These factors determine if a wave group's energy is reflected, absorbed or allowed to propagate. An estimate of the spectrum of gravity waves that reach the level of heating is found by applying ray-tracing to many combinations of frequencies and wavenumbers.

In Chapter IV, the results of Chapters II and III along with some ideas of Stull (1976) are used to calculate a lower boundary condition for the model developed in Chapter V. This model uses equations developed by Bretherton (1966) which are solved by a method described by Chapman and Lindzen (1970).

In Chapter VI, the heating rates are calculated and presented and finally, Chapter VII presents conclusions and recommendations for future work.

CHAPTER II. AN ANALYSIS OF THE SOUNDING OF AUGUST 28, 1976

A study of internal gravity waves excited by intense tropospheric convection should begin with a study of the thunderstorms themselves. On August 28, 1976, showers and thunderstorms passed through Wallops Island, Va. The first precipitation was recorded at 0700 GMT (3 AM local time) but the thunderstorm was strongest from 1100 to 1300 GMT (7 to 9 AM local time) during which 1.1 inches of rain fell. No more thunder was heard after 1300 GMT (9 AM local time) although the precipitation continued to be heavy at times and three quarters of an inch of rain fell from then until the showers tapered off around 1700 GMT (1 PM local time). The thunderstorm that was reported at Wallops Island, Va. was part of a group of thunderstorms and shower activity kicked off by a short wave trough aloft passing through the area. They formed primarily over the Delmarva penninsula.

Figure 2 is a vertical plot of the temperature and dewpoint of the air above Wallops Island at 1200 GMT (8 AM local time) on August 28, 1976. The temperatures have been plotted on a skew T-log p diagram. The sounding is seen to be quite unstable with a deep layer of moist air. This sounding will be used to determine an estimate of an air parcel's vertical velocity as it penetrates a stable region and the length of time it spends in the stable region before its energy is exhausted.

The level at which moist air becomes saturated by adiabatic ascent, the lifting condensation level (LCL), is found to be 900 millibars on this sounding. Above this level, as the saturated parcel travels up through the atmosphere, it will follow the saturated adiabat (process curve in Figure 2) on the aerological diagram. The saturated adiabat

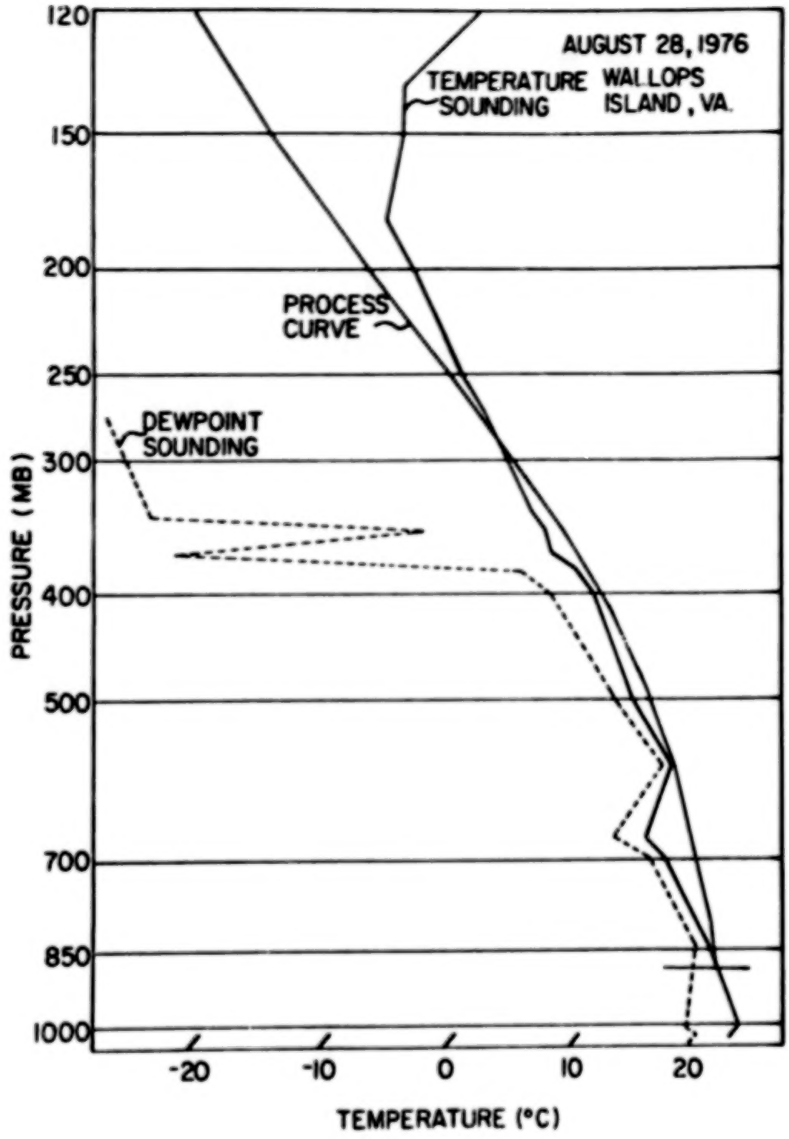

Figure 2. Temperature sounding at Wallops Island, Va. for 1200 Z, August 28, 1976.

shows how the parcel's temperature changes as it ascends. A saturated parcel's temperature will not decrease as fast as the temperature of an unsaturated parcel since the process of condensing water vapor into a liquid releases heat. The saturated adiabats are constructed on the chart with the assumption that all the condensed water vapor falls out of the system as soon as it is produced. Also assumed in this analysis of the sounding are the restrictions of the parcel method which is a method for testing the instability of a parcel of air. The assumptions of the parcel method are:

1. the parcel's movements do not disturb the environment,
2. the parcel only moves adiabatically,
3. the pressure of the parcel equals the pressure of the environment at every level and
4. the parcel does not mix with the environment.

The last assumption is easily recognized as a poor one since only one look at the sides and top of a growing cumulus cloud provides evidence of turbulent mixing. This mixing brings outside air into the parcel in a process known as entrainment. In an attempt to reduce this source of error, the graphical correction technique for entrainment described by Iribarne and Godson (1973) is used. The rate of entrainment is difficult to determine. It depends on the size of the cloud, its stage of development and the velocities of its ascending air currents. In this case, it is assumed that at each step in the graphical technique, the parcel is diluted by ten percent through mixing with external air.

The sample air parcel begins its journey at the LCL. Above this level, the parcel is warmer than the environment, work is done on the

parcel by buoyancy forces and it accelerates. Eventually, it reaches a level at which its temperature equals the temperature of the environment called the equilibrium level (EL). In this case, the EL is 9.5 kilometers (285 mb).

On a skew T-log p diagram, the area between two curves defining the state of the environment and the parcel and the initial and final pressure levels is proportional to the amount of work done on or by the parcel. In this case, between the LCL and the EL, the parcel is warmer than the environment and rises, so the environment is doing work on the parcel. The area on this diagram is a function of the pressure at the EL (285 mb) and the LCL (900 mb) and the mean temperature throughout the layer for the parcel (266°K) and the environment (265°K). The proportionality constant relating the area and the work per unit mass done on the parcel is the universal gas constant R (287 $Jkg^{-1}K^{-1}$). The work per unit mass is calculated to be 330 Jkg^{-1}. It is assumed that all the energy gained by the parcel is transformed into kinetic energy and futhermore, that all the kinetic energy is associated with the parcel's vertical velocity at the EL. With these assumptions, a vertical velocity of 25.7 ms^{-1} is calculated for that parcel.

Above the equilibrium level, the parcel becomes cooler than the environment, the buoyancy forces become negative and the parcel decelerates. To calculate the height to which the parcel penetrates before it exhausts its energy supply, use is made of an equation relating acceleration to the buoyancy of the parcel.

$$\frac{dw}{dt} = \frac{g(T_p - T_e)}{T_e} \qquad (2.1)$$

w is the vertical velocity, g is the acceleration due to gravity, T_p is the temperature of the parcel and T_e is the temperature of the environment. By making use of the fact that dw/dt is equivalent to wdw/dz and integrating both sides, an expression for w as a function of height z is obtained.

$$\frac{w^2(z) - w^2(EL)}{2} = g\int_{EL}^{z} \frac{T_p - T_e}{T_e}\, dz \qquad (2.2)$$

Using the sounding and successive applications of Simpson's Rule, a profile of w with height is calculated and it is discovered that this parcel stops rising (w becomes zero) at 12.5 km. With this w profile it is possible to integrate the expression dt = dz/w(z) by again using Simpson's Rule. The time the parcel is above the equilibrium level is calculated in this manner to be six minutes.

Both the parcel's vertical velocity and the length of time it spends above the equilibrium level will be used later to compute the size of the impulse provided by the convection that excites vertically propagating internal gravity waves that in turn heat the mesosphere. First, it is necessary to derive some basic relations used to describe the propagation of internal gravity waves.

CHAPTER III. GRAVITY WAVES AND RAY-TRACING THEORY

In this chapter, simple equations describing some characteristics of internal gravity waves are derived. They are then used to determine the paths followed by vertically propagating wave groups. This allows the spectrum of gravity waves that reach the level of heating to be determined.

A dispersion equation relating the frequency of a wave to its wavenumber can be derived for internal gravity waves. However, some simplifying assumptions must be made. To begin with, the atmosphere will be considered incompressible. An incompressible atmosphere filters out the high-frequency acoustic wave solutions from the wave equation and leaves the lower frequency gravity wave solutions. Although an incompressible medium may seem unrealistic, equations with this simplification have been found to adequately describe gravity wave motions observed in the real atmosphere (Gossard and Hooke, 1975).

This atmosphere will also be isothermal, isentropic, hydrostatic and non-rotating. Because of the last condition, the Coriolis force, an apparent force appearing in the equations of motion because of the earth's rotation, may be ignored. The Coriolis force is a weak deflecting force that is effective only over a long period of time. Only periods on the order of less than one hour will be considered here so it is reasonable to neglect this force. With these simplifications and assuming two-dimensional propagation in the x-z plane, the set of equations is:

$$\frac{du}{dt} = -\frac{1}{\rho}\frac{\partial p}{\partial x} \tag{3.1}$$

$$\frac{dw}{dt} = - g - \frac{1}{\rho} \frac{\partial p}{\partial z} \tag{3.2}$$

$$\frac{d\rho}{dt} = 0 \tag{3.3}$$

$$\frac{\partial u}{\partial x} + \frac{\partial w}{\partial z} = 0 \quad . \tag{3.4}$$

For an explanation of all symbols, see the List of Symbols on page vii.

Equation (3.1) is the equation for the horizontal component of motion and Equation (3.2) is the vertical equation of motion. Equation (3.3) is an equation representing the incompressibility of the fluid and Equation (3.4) is the incompressible continuity equation.

Equations (3.1) through (3.4) are now linearized by employing the well-known perturbation method. Using this method, the dependent variables are expressed as the sum of a mean component and a small perturbation from that mean. In this case:

$$p = \bar{p}(z) + p'(x,z,t)$$
$$\rho = \bar{\rho}(z) + \rho'(x,z,t)$$
$$u = \bar{u} + u'(x,z,t)$$
$$w = \bar{w} + w'(x,z,t) \quad .$$

The bar denotes a mean quantity and the prime a perturbation. $\bar{w}$ is assumed to be zero and $\bar{u}$, $\bar{\rho}$ and $\bar{p}$ are assumed constant with time t and horizontal distance x. $\bar{u}$ is also constant with height z but $\bar{\rho}$ and $\bar{p}$ are allowed to change with height as in an isothermal atmosphere. An

important assumption of the perturbation method is that the product of two perturbation quantities is assumed to be negligible and may be dropped from the equation. Applying the perturbation method to Equations (3.1) - (3.4) and letting $\bar{u} = U$, a new set of linear equations in the perturbation variables is obtained.

$$\bar{\rho}\left[\frac{\partial u'}{\partial t} + U\frac{\partial u'}{\partial x}\right] = -\frac{\partial p'}{\partial x} \tag{3.5}$$

$$\bar{\rho}\left[\frac{\partial w'}{\partial t} + U\frac{\partial w'}{\partial x}\right] = -g\rho' - \frac{\partial p'}{\partial z} \tag{3.6}$$

$$\frac{\partial \rho'}{\partial t} + U\frac{\partial \rho'}{\partial x} + w'\frac{\partial \bar{\rho}}{\partial z} = 0 \tag{3.7}$$

$$\frac{\partial u'}{\partial x} + \frac{\partial w'}{\partial z} = 0 \tag{3.8}$$

By dividing Equation (3.7) by $\bar{\rho}$ and multiplying by g, the third term becomes

$$w'\frac{g}{\bar{\rho}}\frac{\partial \bar{\rho}}{\partial z} = -N^2 w' \quad . \tag{3.9}$$

N^2 is the symbol for the square of the Brunt-Väisälä frequency. In an incompressible atmosphere, $N^2 = -(g/\bar{\rho})\partial\bar{\rho}/\partial z$. As stated in the introduction, the Brunt-Väisälä frequency is the frequency at which a parcel will oscillate if displaced adiabatically an infinitesimal distance Δz. Thus Equation (3.7) becomes

$$\frac{g}{\bar{\rho}}\frac{\partial \rho'}{\partial t} + \frac{g}{\bar{\rho}} U \frac{\partial \rho'}{\partial x} - N^2 w' = 0 \quad . \tag{3.10}$$

Since the motions to be investigated are wave-like, the perturbation variables will be expressed in the forms

$$u' = \tilde{U}\exp[i(\omega t - kx - mz)] \tag{3.11}$$

$$w' = \tilde{W}\exp[i(\omega t - kx - mz)] \tag{3.12}$$

$$\frac{\rho'}{\bar{\rho}} = \tilde{R}\exp[i(\omega t - kx - mz)] \tag{3.13}$$

$$\frac{p'}{\bar{\rho}} = \tilde{P}\exp[i(\omega t - kx - mz)] \tag{3.14}$$

where only the real parts of the right sides are of interest. k is the wavenumber in the x direction and m is the wavenumber in the z direction. This form assumes sinusoidal variations in time and in the horizontal and vertical directions. Substituting (3.11) - (3.14) into equations (3.5), (3.6), (3.10) and (3.8) and noting that the term $\exp[i(\omega t - kx - mz)]$ will be common to all terms and drop out, the following are obtained:

$$(\omega - kU)\tilde{U} - k\tilde{P} = 0 \tag{3.15}$$

$$i(\omega - kU)\tilde{W} + g\tilde{R} - im\tilde{P} = 0 \tag{3.16}$$

$$i(\omega - k\tilde{U})g\tilde{R} - N^2\tilde{W} = 0 \tag{3.17}$$

$$k\tilde{U} + m\tilde{W} = 0 \quad . \tag{3.18}$$

In matrix form, these equations look like this:

$$\begin{bmatrix} \omega-kU & 0 & -k & 0 \\ 0 & i(\omega-kU) & -im & g \\ k & m & 0 & 0 \\ 0 & -N^2 & 0 & i(\omega-kU)g \end{bmatrix} \begin{bmatrix} \tilde{U} \\ \tilde{W} \\ \tilde{P} \\ \tilde{R} \end{bmatrix} = 0 \quad . \tag{3.19}$$

A trivial solution to this set of equations would be $\tilde{U} = \tilde{W} = \tilde{P} = \tilde{R} = 0$. For a non-trivial solution to exist, the determinant formed by the coefficients must equal zero. When the equation formed by calculating the determinant and setting it equal to zero is solved for the frequency ω, the result is the dispersion relation:

$$\omega = kU \pm N \left\{ \frac{k^2}{k^2 + m^2} \right\}^{1/2} \quad . \tag{3.20}$$

When two or more waves with slightly differing frequencies and wavenumbers propagate at the same time through a medium, they interact to form an interference pattern in their amplitudes. These patterns are referred to as wave groups or modulation envelopes. The wave groups propagate at the group velocity, a speed different from the speed of an individual wave. The group velocity can be thought of as the speed

at which energy is transmitted by the waves. It is equal to the frequency differentiated with respect to the wavenumber. In this case, using Equation (3.20), the group velocity in the x direction is:

$$u_g = \frac{\partial \omega}{\partial k} = U \pm N\left[\frac{m^2}{(k^2 + m^2)^{3/2}}\right] \quad . \tag{3.21}$$

In the z direction, the group velocity is:

$$w_g = \frac{\partial \omega}{\partial m} = \pm N\left[\frac{km}{(k^2 + m^2)^{3/2}}\right] \quad . \tag{3.22}$$

Bretherton (1966) has shown how equations (3.20), (3.21) and (3.22) can be used to calculate the path that a certain wave group with a dominant frequency and wavenumber will follow as it moves through an atmosphere in which both U and N change with height. For these raypaths to be valid, the waves and the atmosphere must obey the WKB approximation. That is, the vertical wavelength should be small compared to the height over which the horizontal wind U and the Brunt-Väisälä frequency N change significantly. In this atmosphere, u_g and w_g will change with height also.

Bretherton produces the important result that following a wave group at its local group velocity, the dominant frequency and horizontal wavenumber by which the wave group is identified will remain constant. By calculating the vertical wavenumber m from Equation (3.20) at even intervals (every kilometer in this case) using local values of U and N and a constant ω and k, it is possible to determine the vertical

profile of m. Equations (3.21) and (3.22) can then be solved for the group velocities at each level using local values of m, U and N. The time it takes the wave group to reach each new level is computed from the local group velocity and the distance between levels (1 kilometer). The distance downwind that the wave group travels can be computed using the local horizontal group velocity. In this way, the information needed to plot the paths the wave groups travel, their raypaths, is obtained. The raypaths are calculated up to 85 km. Figure 3 shows the raypaths of several wave groups.

All the waves propagating upwards through the atmosphere do not necessarily reach its uppermost regions. Many are affected by reflection and critical levels.

If the Doppler-shifted frequency, $\omega - kU$, equals the local value of the Brunt-Väisälä frequency N, the raypath becomes vertical and the group is reflected down towards the ground. An example of this is shown in Figure 3.

A wave group's critical level is the level at which its Doppler-shifted frequency is equal to zero. In the vicinity of a critical level, the vertical group velocity becomes proportional to the square of the distance from it and the wave takes an infinite time to reach it (Bretherton, 1966). Thus, the energy of the wave can't be transmitted through this level and is absorbed there.

Critical levels and reflection are important to consider since their existence or non-existence determines which gravity waves can reach the mesosphere. This means that the background wind measurements are extremely important since they play a role in calculating the Doppler-shifted frequency. Whether a critical level exists or not

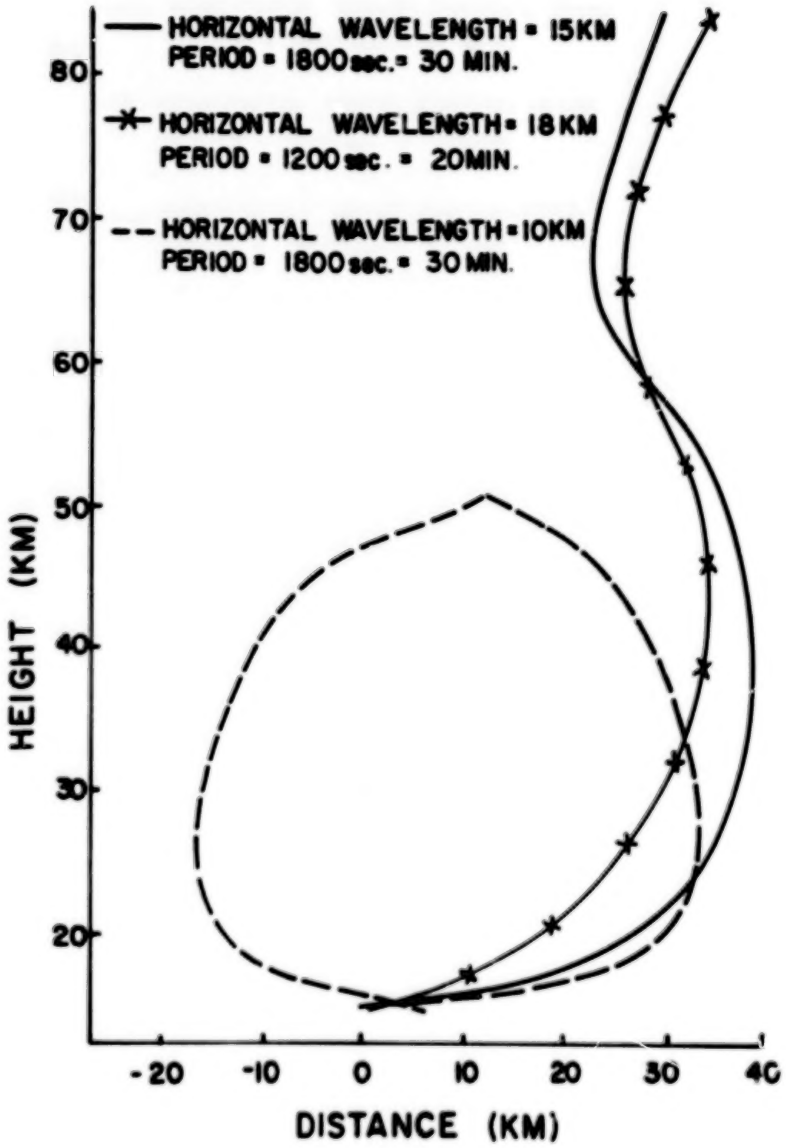

Figure 3. Raypaths of gravity wave groups initiated at 15 km on August 28, 1976.

can depend on a difference in the wind speed of only a few meters per second. Therefore, absolute statements cannot be made about the spectrum of gravity waves reaching a certain level unless one is certain of the accuracy of his wind measurements. However, general conclusions may be reached about the size of the spectrum if the paths of many waves with different frequencies and wavenumbers are studied. This has been done and Figure 4 is a plot of the fate of gravity waves of different frequencies and wavenumbers (plotted as periods and horizontal wavelengths) in the atmosphere of August 28, 1976. This plot will be used in the next chapter to determine the range of frequencies and wavenumbers that can penetrate this atmosphere to the level of heating.

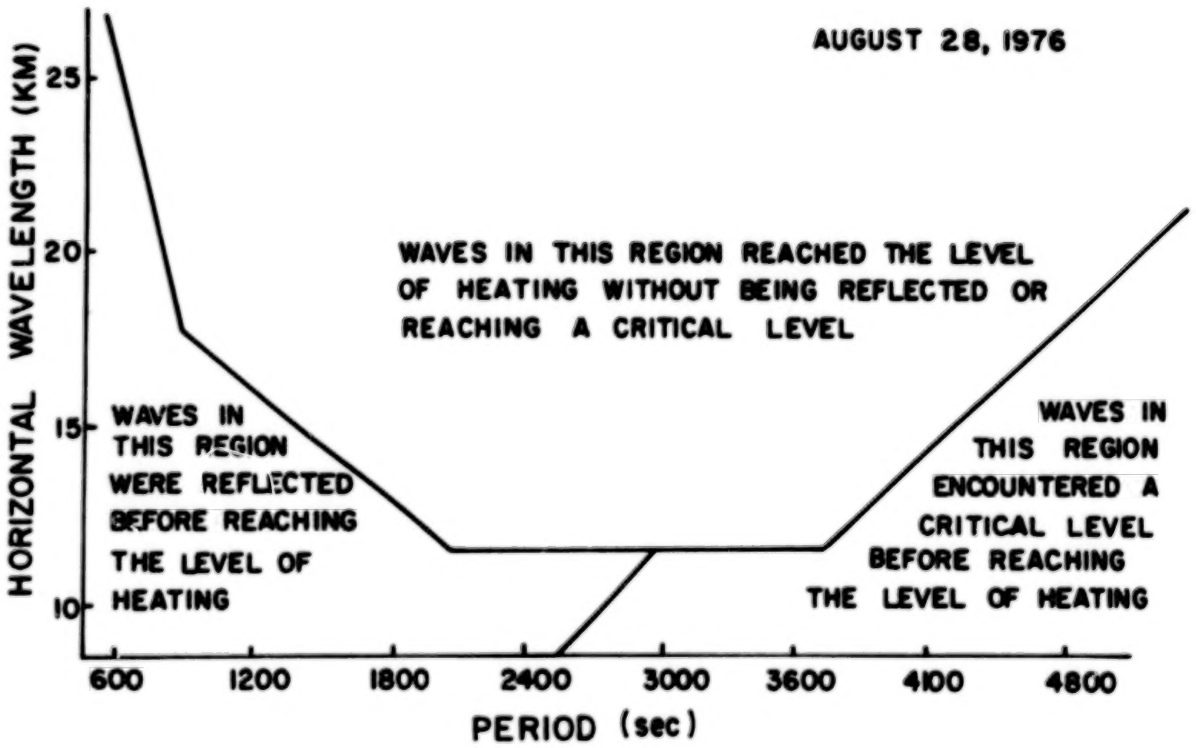

Figure 4. Fate of gravity wave groups identified by dominant wavelength and periods in atmosphere of August 28, 1976.

CHAPTER IV. CALCULATION OF THE CONVECTIVE ENERGY INPUT

In Chapter II, it was shown that a parcel rising in unstable air reaches an equilibrium level and then penetrates a distance into a stable layer, before sinking back down. This type of behavior has been studied in the context of thermals overshooting the atmospheric boundary layer into an overlying temperature inversion and has been labeled penetrative convection. Stull (1976) has studied this type of penetrative convection and many of his ideas can be applied to describe the penetrating elements found in a thunderstorm.

Stull has developed a useful representation of an idealized convective element. See Figure 5. A parcel penetrates a distance d into a stable region and then sinks back to the equilibrium level. Figure 5a represents the parcel's height above the equilibrium level as a sinusoidal function of time. P/2 is the time the parcel is above the equilibrium level, calculated in Chapter II to be six minutes. Figure 5b is the idealized element at the time of maximum penetration as a function of distance x. The figure shows that some of the stable air is drawn down below the equilibrium level to conserve mass. D is the diameter of the element at the equilibrium level.

In the real atmosphere, thunderstorm updrafts acting as penetrative elements excite internal gravity waves with a broad range of frequencies and wavenumbers. The irregularities of the individual elements make the precise determination of the frequencies and wavenumbers difficult. Stull solves this problem by making a harmonic analysis of his idealized disturbance. He comes up with a smooth, almost Gaussian frequency spectrum and an equally simple shape for the wavenumber spectrum. Both are shown in Figure 6.

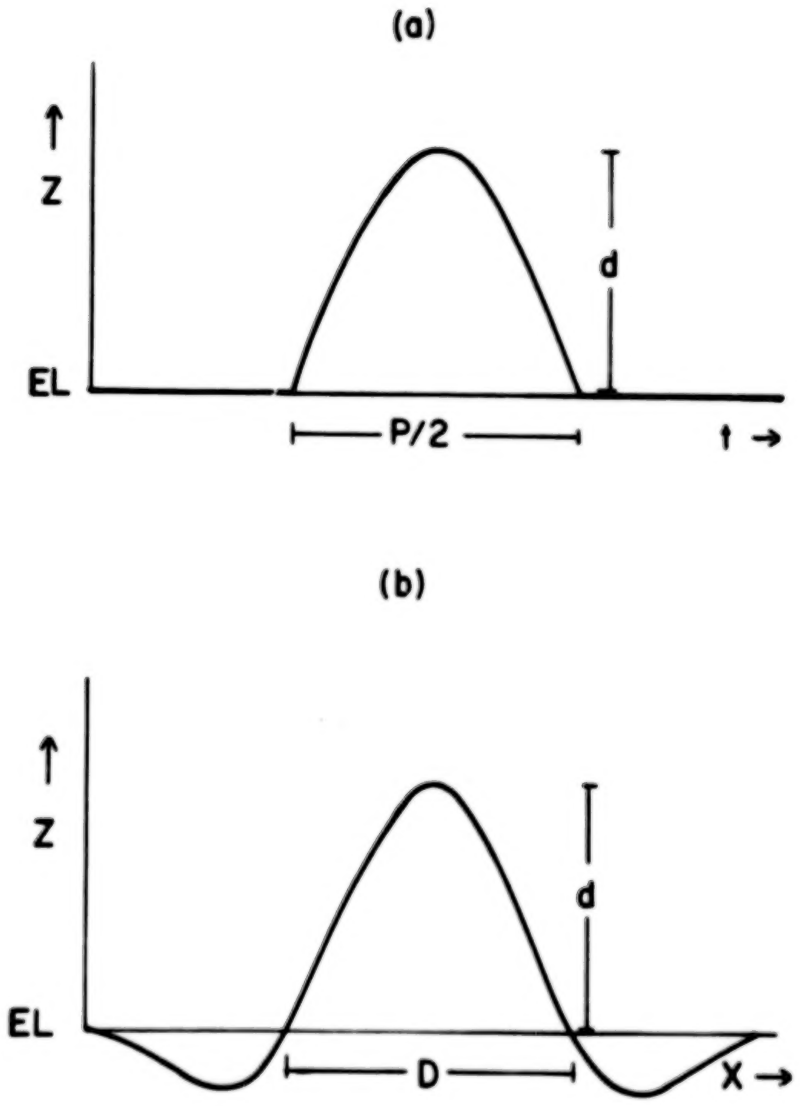

Figure 5. Idealized penetrative element (a) as a function of time and (b) as a function of distance.

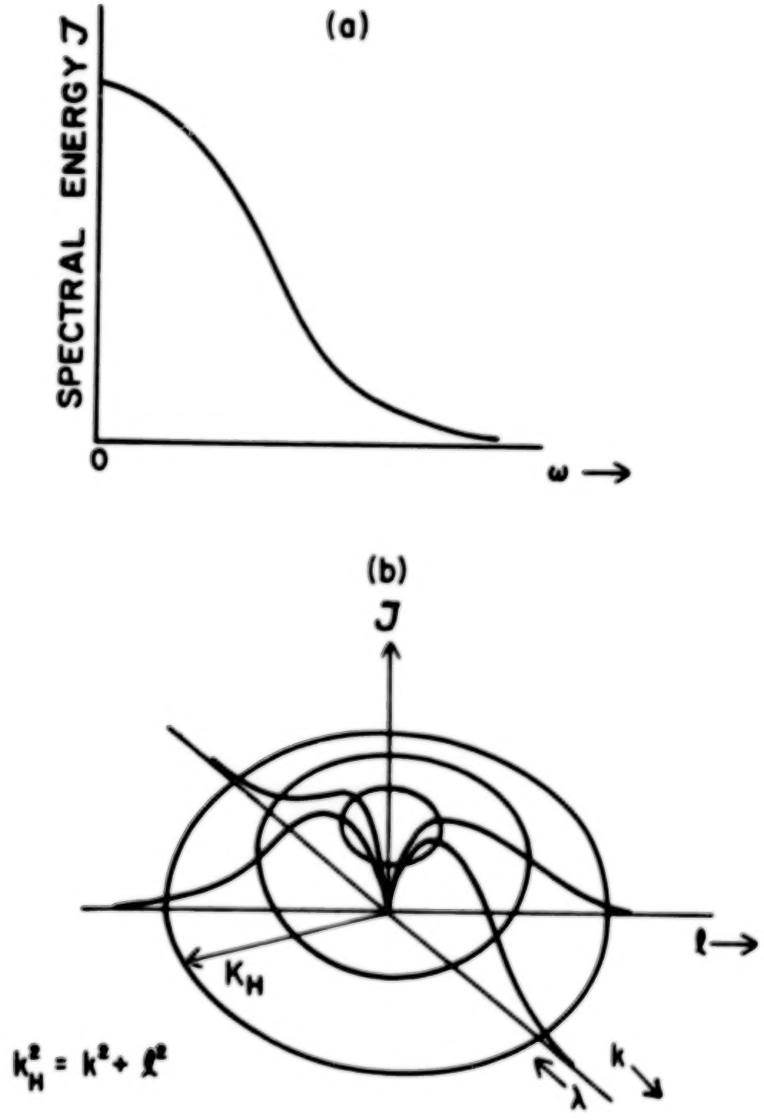

Figure 6. Spectral energy density J as a function of (a) frequency and (b) wavenumber.

Note from the frequency spectrum that the bulk of the energy is associated with low-frequency or longer period waves. From the wavenumber spectrum it is not as easy to see with which wavenumbers most of the energy is associated but there is a wavelength at which the energy density is a maximum and that may be calculated.

Stull combines the equations describing the shapes in Figure 6 to obtain an expression for the spectral energy density J of one idealized convective element.

$$J = \frac{k_H}{2^{1/2}\pi^{3/2} f \kappa_H^2} \exp - \frac{1}{2}\left(\frac{\omega_i^2}{f^2} + \frac{k_H^2}{\kappa_H^2}\right) \quad , \tag{4.1}$$

where $f \equiv 2\pi/P$ and $\kappa_H \equiv \pi/D$. ω_i is the Doppler-shifted frequency and k_H is the horizontal wavenumber ($k_H^2 = k^2 + \ell^2$ where $k(\ell)$ is the wavenumber in the x(y) direction). J is normalized so that

$$\int_{\phi=0}^{2\pi} \int_{k_H=0}^{\infty} \int_{\omega_i=0}^{\infty} J d\omega_i dk_H d\phi = 1 \quad . \tag{4.2}$$

ϕ is the horizontal angle in wavenumber space.

If the normalized energy density function (Equation (4.2)) is integrated over a range of wavenumbers and frequencies corresponding to the wavelengths and periods of the range of waves calculated to reach the level of heating by ray-tracing theory, the result will be a rough estimate of the fraction of the total kinetic energy of the parcel that is used to excite those gravity waves at the equilibrium level.

The mean value theorem is used to integrate the expression

$$\int_{\phi}\int_{k_H}\int_{\omega_i} J\,d\omega_i\,dk_H\,d\phi = \bar{J}\Delta\omega_i\Delta k_H\Delta\phi \quad . \tag{4.3}$$

$\bar{J}$ is a mean value of the energy density function, $\Delta\omega_i$ is the frequency interval and Δk_H is the horizontal wavenumber interval. Since the energy density function J is integrated over all horizontal angles in wavenumber space, $\Delta\phi$ equals 2π. The next step is to calculate Δk_H and $\Delta\omega_i$ with the help of Figures 4 and 6.

The wavenumber at which the energy density function is a maximum (the peak of the graph in Figure 6b) is calculated from Equation (4.1) to be $k_H = \pi/D$. In terms of horizontal wavelength ($\lambda_H = 2\pi/k_H$), the wavelength at maximum J is equal to 2D. Assuming the diameter of the element at the equilibrium level is one kilometer, the wavelength for maximum J is two kilometers. Combining this fact with the information gathered from Figure 4 that wavelengths less than twelve kilometers do not reach the level of heating and noting that wavelength increases toward the origin in Figure 6b, it can be seen that the range of wavelengths contributing the energy to the heating, Δk_H, will be found to the left of the peak and that twelve kilometers is the right edge (or short-wavelength side) of the range.

The chart in Figure 4 shows that the long-wavelength side of the wavelength range is not easily defined. All the longer wavelengths combined with the range of frequencies that can be considered reach the level of heating, although Figure 6b shows that little energy is

associated with the very long wavelengths. There are two reasons for no cut-off. First, the larger the wavelength, the smaller the wavenumber and therefore the Doppler-shifted frequency (ω-kU) will never be zero (with the range of frequencies considered here). Thus, a critical level will never be reached. Also, a small wavenumber means that even with the strong easterly winds of the stratosphere, the Doppler-shifted frequency, ω_i, will always be less than the Brunt-Väisälä frequency and the wave group will not be reflected.

Since no cut-off on the small-wavenumber side of Figure 6b is indicated from ray-tracing theory, the wavenumber interval is estimated to range from the clearly defined edge at the wavenumber associated with a wavelength of 12 kilometers all the way down to the origin (wavenumber equal to zero). Therefore, Δk_H is approximately 0.5 km^{-1}.

The frequency interval, $\Delta\omega_i$, can be estimated from Figure 4 by looking at the area on the figure associated with the most energy for the wavelength range and assuming the frequency range there. This range taken at wavelength equal to 12 kilometers is 0.0013 sec^{-1}.

The fractional part of the energy density associated with the range of gravity waves that reach the mesosphere is found by calculating the right side of Equation (4.3) using the values for $\Delta\omega_i$ and Δk_H just estimated. The fraction is 0.0021. If the total energy associated with the rising parcel calculated in Chapter II from the temperature sounding of August 28 is multiplied by this fraction, the result is the amount of energy associated with the range of gravity waves that reach the level of heating. The assumptions that this energy is all converted into kinetic energy and all the kinetic energy is associated with a vertical velocity are made. Therefore,

$$KE = \frac{1}{2} w^2 \qquad (4.4)$$

where KE represents the fractional kinetic energy per unit mass ($0.7 Jkg^{-1}$). From Equation (4.4), a vertical velocity of $1.2\ ms^{-1}$ is calculated.

The kinetic energy associated with a vertical velocity of $1.2\ ms^{-1}$ represents an estimate of the energy initially contained by those waves calculated to reach the mesosphere by ray-tracing theory. By using this value as the impulse that generates the internal gravity waves in a model, the energy attenuation by reflection and critical level interaction of waves on their way to the mesosphere will be accounted for. Therefore the calculated heating will be representative of the actual energy involved.

CHAPTER V. THE MODEL OF GRAVITY WAVE STRUCTURE

The equations used to find the detailed gravity wave structure are taken from Bretherton (1966). They are derived assuming a compressible atmosphere, but the equations describing the propagation of wave groups derived previously for an incompressible atmosphere may be used in conjunction with them as long as the WKB approximation is valid. Also, the Brunt-Väisälä frequency is now expressed as a function of the change of potential temperature with height.

$$N^2 = \frac{g}{\theta} \frac{d\theta}{dz} \tag{5.1}$$

The linearized equations corresponding to such an atmosphere are reproduced from Bretherton (1966).

$$\frac{D}{Dt} u' + U_z w' + \frac{1}{\rho} p_x' = 0 \tag{5.2}$$

$$\frac{D}{Dt} w' + \frac{g\rho'}{\rho} + \frac{1}{\rho} p_z' = 0 \tag{5.3}$$

$$\frac{1}{\rho} \frac{D}{Dt} \rho' + \frac{1}{\rho} \rho_z w' + u_x' + w_z' = 0 \tag{5.4}$$

$$\frac{g}{\gamma p} \frac{D}{Dt} p' - \frac{g}{\rho} \frac{D}{Dt} \rho' = N^2 w' \tag{5.5}$$

x or z used as a subscript denotes partial differentiation with respect to that variable. $\frac{D}{Dt}$ stands for the operator $\frac{\partial}{\partial t} + U \frac{\partial}{\partial x}$ and $\gamma = c_p/c_v$.

In these equations, ρ is a local value of the background density and is a function of height. It is the exponential variation of ρ that allows the amplitude of the waves to grow with height as a result of the conservation of energy. Bretherton rescales the equations to account for this effect by naming a reference density $\bar{\rho}$. He defines new variables in this way:

$$(u', w') = (\rho/\bar{\rho})^{-1/2} (\tilde{u},\tilde{w}) \tag{5.6}$$

$$p' = (\rho/\bar{\rho})^{1/2} \tilde{p} \tag{5.7}$$

$$\frac{g\rho'}{\rho} - \frac{gp'}{\gamma p} = (\rho/\bar{\rho})^{-1/2} \tilde{\sigma} \quad . \tag{5.8}$$

Equations (5.2) to (5.5) become

$$\frac{D}{Dt} \tilde{u} + U_z \tilde{w} + \frac{1}{\bar{\rho}} \tilde{p}_x = 0 \tag{5.9}$$

$$\frac{D}{Dt} \tilde{w} + \tilde{\sigma} + \frac{1}{\bar{\rho}} (\frac{\partial}{\partial z} - \frac{1}{H})\tilde{p} = 0 \tag{5.10}$$

$$\frac{1}{c^2} \frac{1}{\bar{\rho}} \frac{D}{Dt} \tilde{p} + \tilde{U}_x + (\frac{\partial}{\partial z} + \frac{1}{H})\tilde{w} = 0 \tag{5.11}$$

$$\frac{D}{Dt} \tilde{\sigma} - N^2\tilde{w} = 0 \quad . \tag{5.12}$$

Here, c is the speed of sound equal to $\gamma p/\rho$ and H is a measure of the scale height such that:

$$\frac{1}{H} = \frac{1}{2\rho}\rho_z + \frac{1}{\theta}\theta_z \quad . \tag{5.13}$$

At this point, c is allowed to approach infinity as in an incompressible atmosphere with the sole effect being the elimination of acoustic wave solutions. This leaves the continuity equation (Eq. 5.11) in the form

$$\tilde{u}_x + \left(\frac{\partial}{\partial z} - \frac{1}{H}\right)\tilde{w} = 0 \quad . \tag{5.14}$$

As a result of eliminating $\tilde{u}$, $\tilde{p}$, and $\tilde{\sigma}$ among Equations (5.9), (5.10), (5.12) and (5.14), the following equation is found:

$$\frac{D^2}{Dt^2}(\tilde{w}_{xx} + \tilde{w}_{zz}) + N^2\tilde{w}_{xx} = \frac{D}{Dt}\left[\left(U_{zz} - \frac{2}{H}U_z\right)\tilde{w}_x\right] + \frac{D^2}{Dt^2}\left[\frac{1}{H^2}(1 + H_z)\tilde{w}\right] \quad . \tag{5.15}$$

The first term on the right-hand side comes from the approximation Bretherton makes that $\tilde{w}_{xz} = -\tilde{w}_x/H$.

By assuming a wave form in the horizontal direction and time with a real wavenumber and frequency, the vertical structure of the wave may be found. Therefore,

$$\tilde{w} = \tilde{w}(z)\exp[i(kx - \omega t)]$$

and the equation becomes:

$$\tilde{w}_{zz} + \tilde{w}\left[-k^2 + \frac{k^2N^2}{(\omega - kU)^2} + \frac{k(U_{zz} - \frac{2}{H}U_z)}{(\omega - kU)} - \frac{1}{H^2}(1 + H_z)\right] = 0 \quad . \tag{5.16}$$

This equation is of the form

$$\tilde{w}_{zz} + f(z)\tilde{w} = 0 \tag{5.17}$$

where f(z) refers to the terms within the brackets and is a function of height.

Although this equation resembles a simple wave equation, the function of height f(z) prevents it from being solved analytically. However, a numerical technique described by Chapman and Lindzen (1970) and originally discussed by Bruce, Peaceman, Rachford and Rice (1953) may be used. This method uses finite difference approximations for the derivatives and incorporates boundary conditions for the top and bottom of the model. The bottom boundary condition is a vertical velocity of 1.2 ms^{-1} at a level of ten kilometers. Ten kilometers is the approximate height of the equilibrium level for a penetrative element on August 28, 1976. A radiation condition is used as the upper boundary condition. It assumes that there are no energy sources at $z = \infty$.

The model's domain extends from 10 km to 80 km and the region is divided into 100-meter-thick layers. This fine resolution is necessary

for numerical reasons (see Chapman and Lindzen, 1970). All the data needed to solve the equation (winds, temperature, scale height, etc.) are calculated or taken directly from the rocket measurements. Linear interpolation is used to find values between measurement levels. The upper level winds are a smoothed profile from wind measurements over several days. See Figure 7.

The equation is solved with a predetermined frequency and horizontal wavenumber. The values for ω and k are only those combinations found to describe wave groups that reach the level of heating.

The resulting values of $\tilde{w}$ are multiplied by the factor in Equation (5.6) to put back the density effect. Values of w', the actual vertical velocity perturbations resulting from the propagation of internal gravity waves of some frequency ω and wavenumber k, are then obtained. A plot of the amplitude of w' (since w' is complex) is shown in Figure 8. It reveals the great effect decreasing density with height has on the structure of the waves.

The horizontal velocity perturbation u' can now be calculated using the continuity equation (Eq. 5.14), since the vertical variation of w' and thus $\tilde{w}$ is now known. A wave form is assumed for $\tilde{u}$ in x and t, i.e., k and ω are made real, so that

$$\tilde{u} = \tilde{u}(z) \exp[i(kx - \omega t)]$$

and Equation (5.14) becomes

$$\tilde{u} = \frac{i}{k} \left(\frac{\partial}{\partial z} - \frac{1}{H}\right) \tilde{w} \quad . \tag{5.18}$$

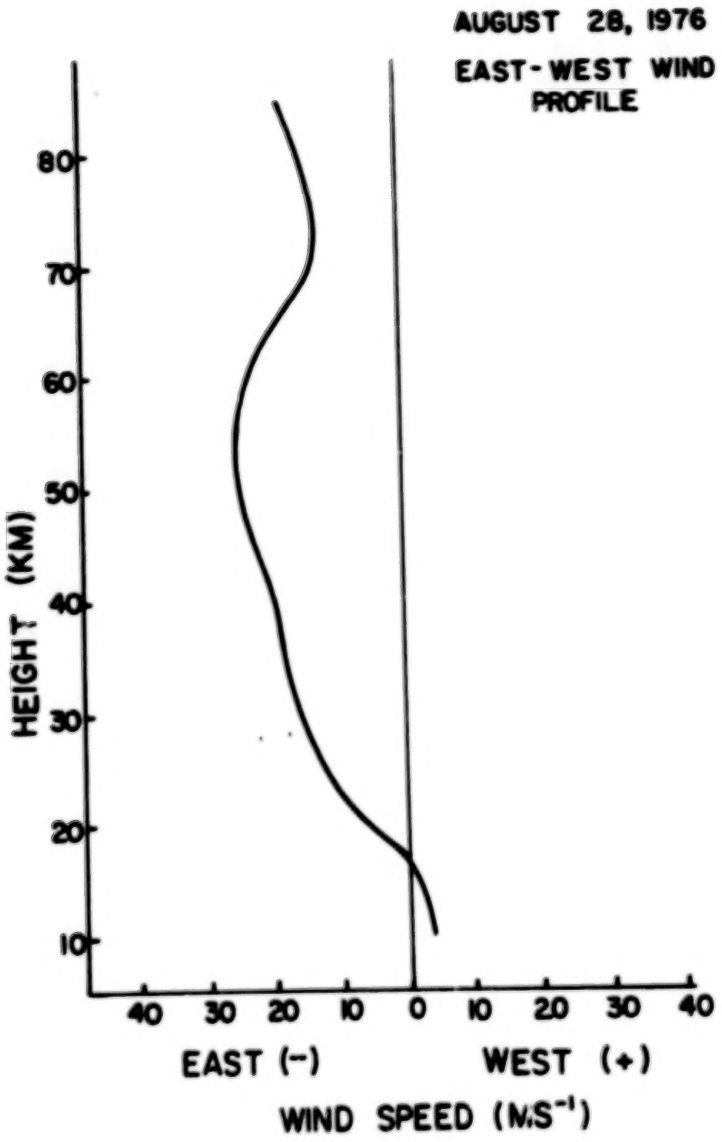

Figure 7. Smoothed east-west wind profile for August 28, 1976 at Wallops Island, Va.

Solving this equation for $\tilde{u}$ and multiplying the result by the factor in Equation (5.6), the horizontal perturbation velocities corresponding to the internal gravity waves are obtained. A plot of the amplitude of u' is shown in Figure 9 in which the density effect on wave amplitudes is also apparent.

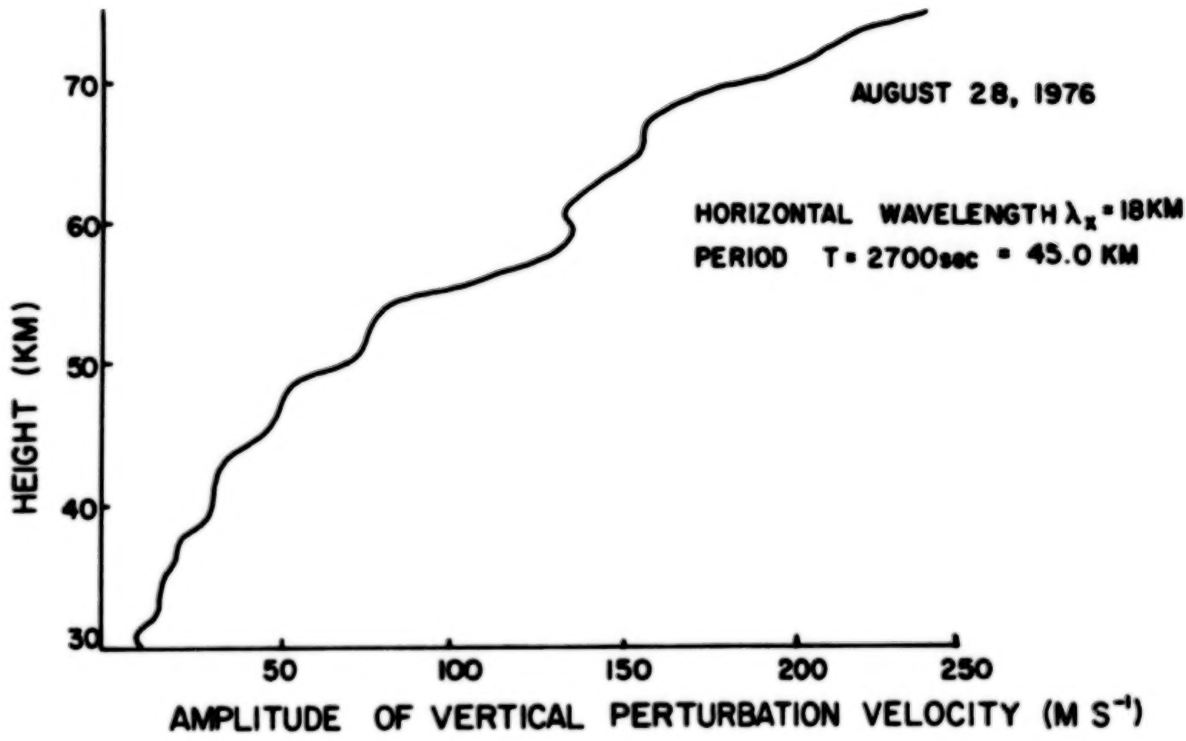

Figure 8. Amplitude of vertical perturbation velocity w' as a function of height.

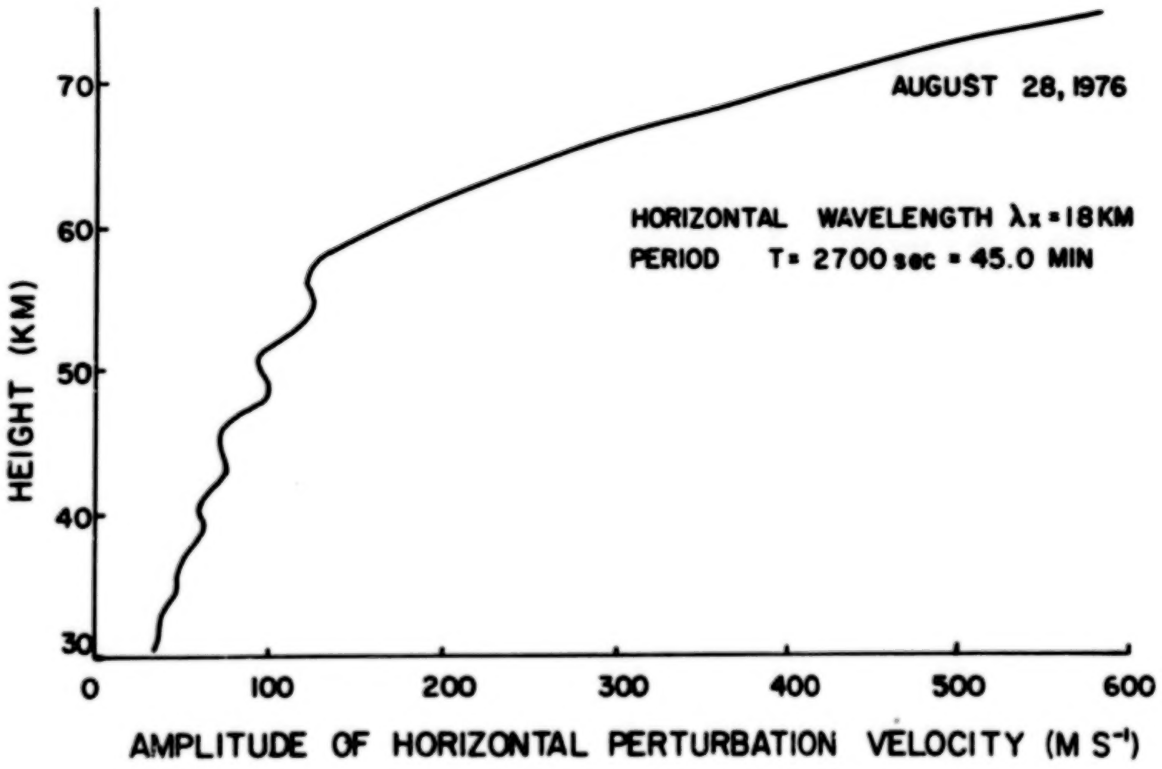

Figure 9. Amplitude of horizontal perturbation velocity u' as a function of height.

CHAPTER VI. CALCULATION OF HEATING RATES

The gravity wave solutions found in Chapter V were obtained without any friction. The rate at which friction would dissipate energy in those solutions is now calculated and it is assumed that this energy heats the background atmosphere.

Gravity waves have been shown to have the potential to produce large amounts of heating. Hines (1965) has studied this effect at heights above the mesopause (80 km). He suggests that heating by gravity waves may be responsible for the rapid rise of temperature with height that occurs in the E-region (100-120 km). Whitaker (1963) has suggested that gravity waves continuously propagating upwards from the photosphere of the sun are responsible for maintaining the high temperature of the solar corona.

In this case, an estimate of just how much of the kinetic energy of these perturbations is destroyed by frictional dissipation is found by assuming that the friction term may be represented by means of an eddy viscosity coefficient K. K is a function of height. Cunnold, Alyea, Phillips and Prinn (1975) developed the profile of K for the stratosphere and mesosphere seen in Figure 10 which will be used here. In this case, the wind varies only in the vertical and the viscous dissipation terms can be represented this way:

$$\frac{\partial}{\partial z}\left(K \frac{\partial u'}{\partial z}\right) \quad \text{and} \quad \frac{\partial}{\partial z}\left(K \frac{\partial w'}{\partial z}\right) \quad .$$

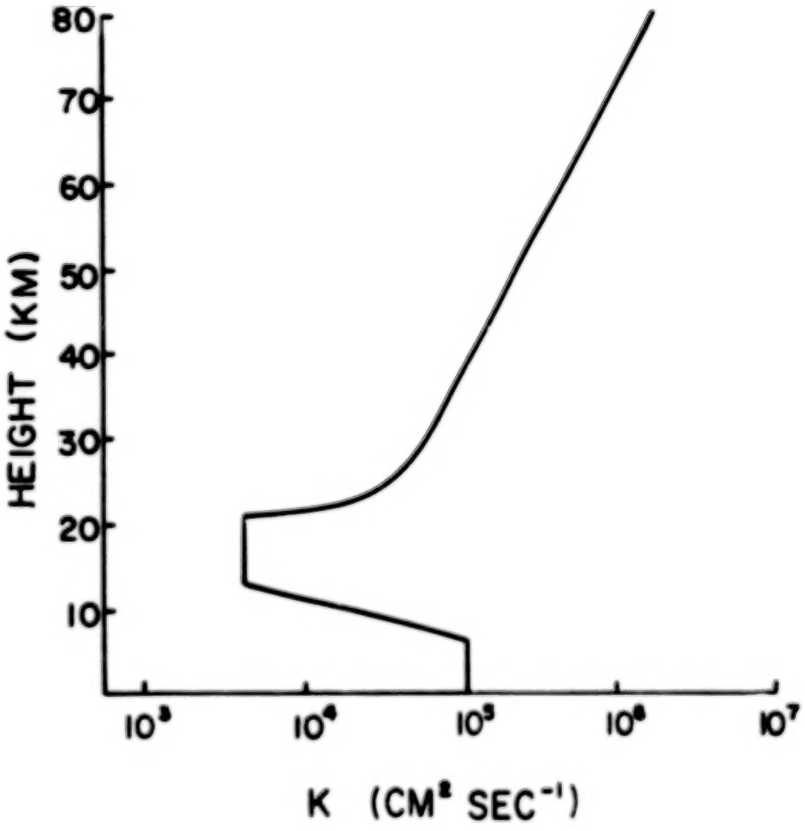

Figure 10. Eddy viscosity coefficient K as a function of height.

In order to determine the rate of destruction of kinetic energy (KE) by these terms, they are multiplied by u' and w' respectively and added.

$$\frac{d\frac{u'^2}{2}}{dt} + \frac{d\frac{w'^2}{2}}{dt} = \frac{d(KE)}{dt} = u' \frac{\partial}{\partial z}\left(K \frac{\partial u'}{\partial z}\right) + w' \frac{\partial}{\partial z}\left(K \frac{\partial w'}{\partial z}\right) \tag{6.1}$$

Next the thermodynamic equation may be employed.

$$\frac{dq}{dt} = c_v \frac{dT}{dt} + p \frac{d\alpha}{dt} \tag{6.2}$$

c_v, a constant, is the specific heat at constant volume and α is the specific volume. The kinetic energy destruction rate is set equal to the heat added per unit time, dq/dt, since it is assumed that all the kinetic energy due to the velocity perturbations caused by gravity waves is dissipated as heat.

In order to obtain a heating rate from this equation, the assumption must be made that all the heat energy per unit time, dq/dt, goes into heating the local medium as represented by the term $c_v dT/dt$ and none into expanding the medium as represented by the term $pd\alpha/dt$, since it is difficult to estimate the amount of heat used in expansion. Therefore, it must be remembered that the heating rates obtained this way (in the form degrees K per day) will be the upper limit of the actual heating possible.

Some results obtained by solving

$$\frac{dT}{dt} = \frac{1}{c_v} \frac{dq}{dt} \tag{6.3}$$

are shown in Figures 11, 12 and 13.

All the procedures performed on the data of August 28 are now used with the data of September 2. Convective activity occurred on that date as a result of a cold front moving through the area.

When raypaths are calculated for wave groups in the atmosphere of September 2, some changes are necessary in the low level wind profile. The sounding for that day at 8 AM local time recorded westerly winds on the order of 30 m/sec at the levels where the waves would be initiated by the penetrative convection. These strong positive winds produce critical levels ($\omega - kU = 0$) for a large range of frequencies and wavenumbers, thus effectively putting a lid on the propagation of most of the wave energy.

Since a sounding only reflects the value of the wind speed at one instant and at one point in space and since penetrative convection was going on all around the area before and after the time of the sounding, it is not unreasonable to assume that the wind can have different values at other times. Therefore, the wind values used in computation of the raypaths have been changed to smaller positive values (~ 5 ms^{-1}) to allow more of the wave groups to reach the mesosphere.

Some heating rates calculated for September 2 may be seen in Figures 14, 15 and 16.

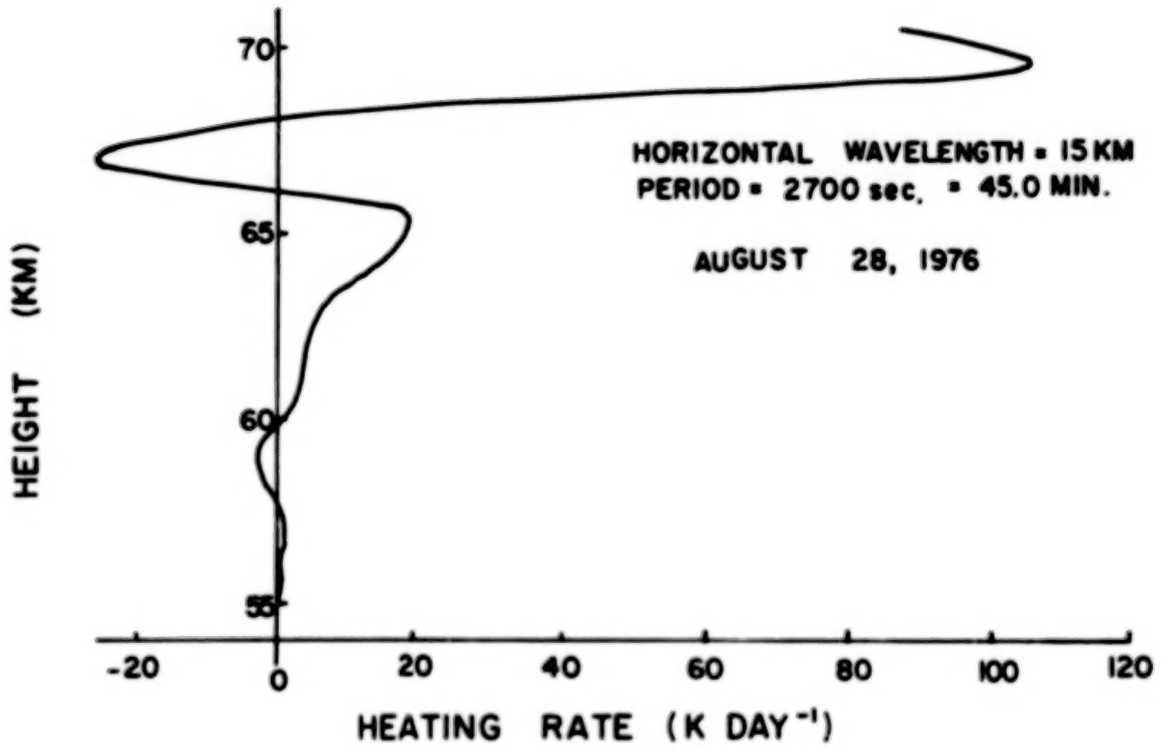

Figure 11. Heating rates as a function of height, August 28, 1976.

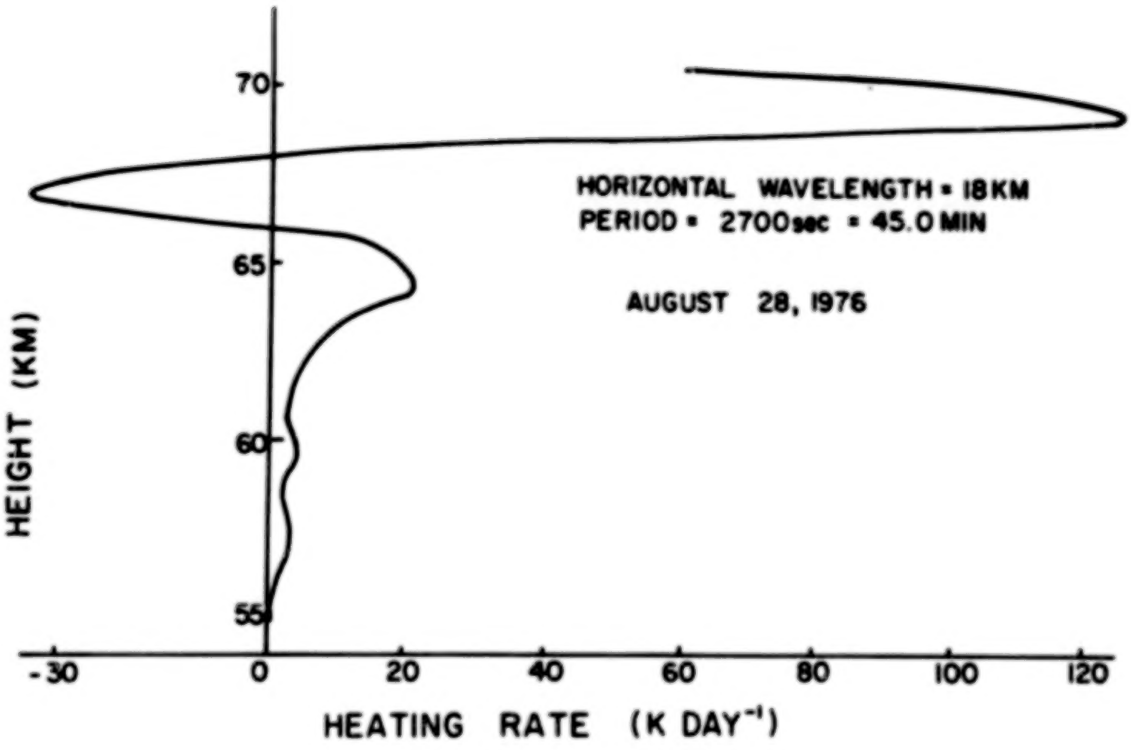

Figure 12. Heating rates as a function of height, August 28, 1976.

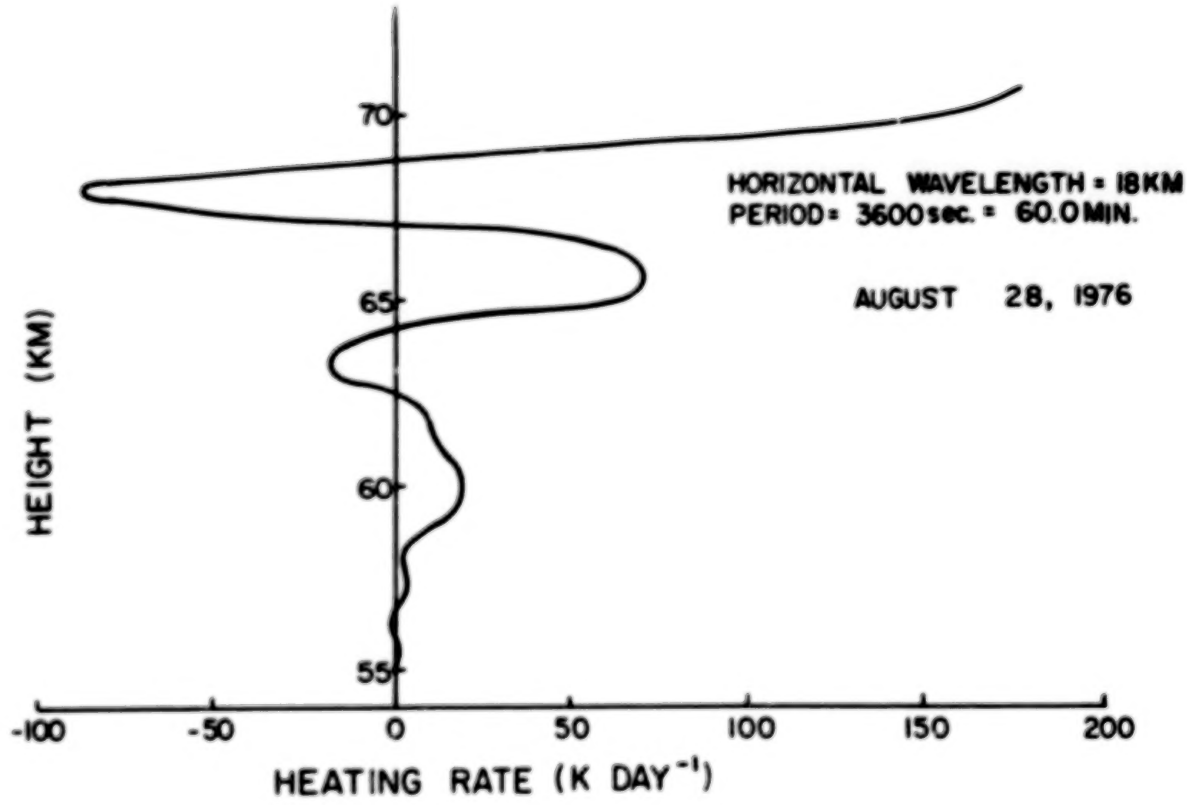

Figure 13. Heating rates as a function of height, August 28, 1976.

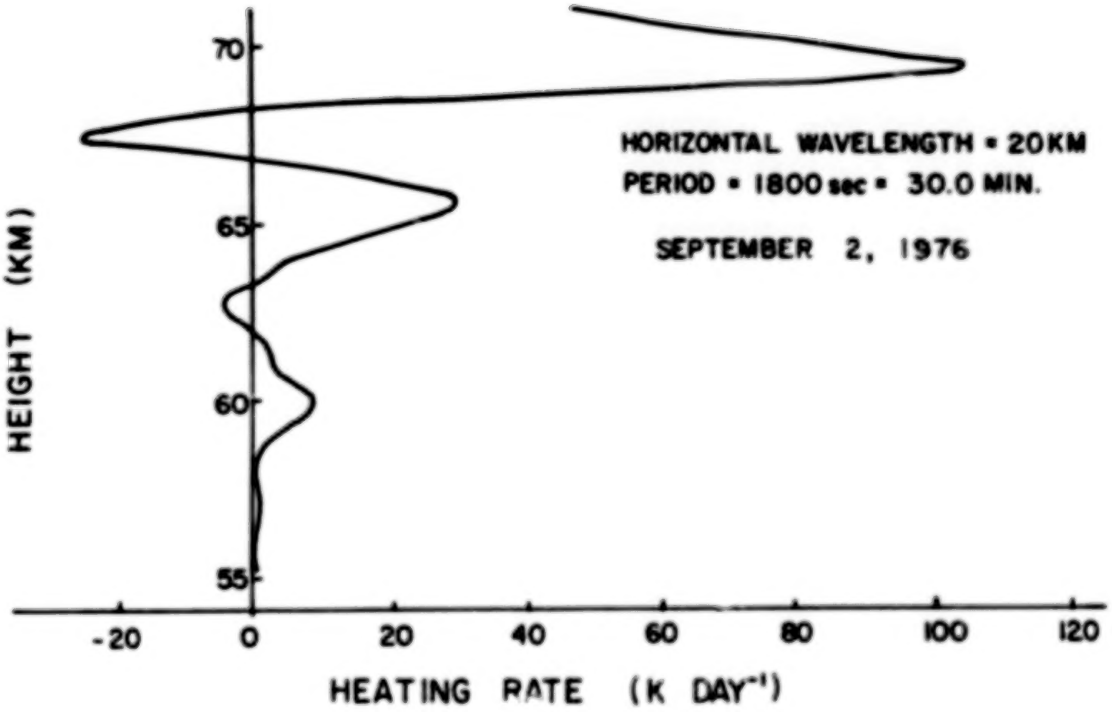

Figure 14. Heating rates as a function of height, September 2, 1976.

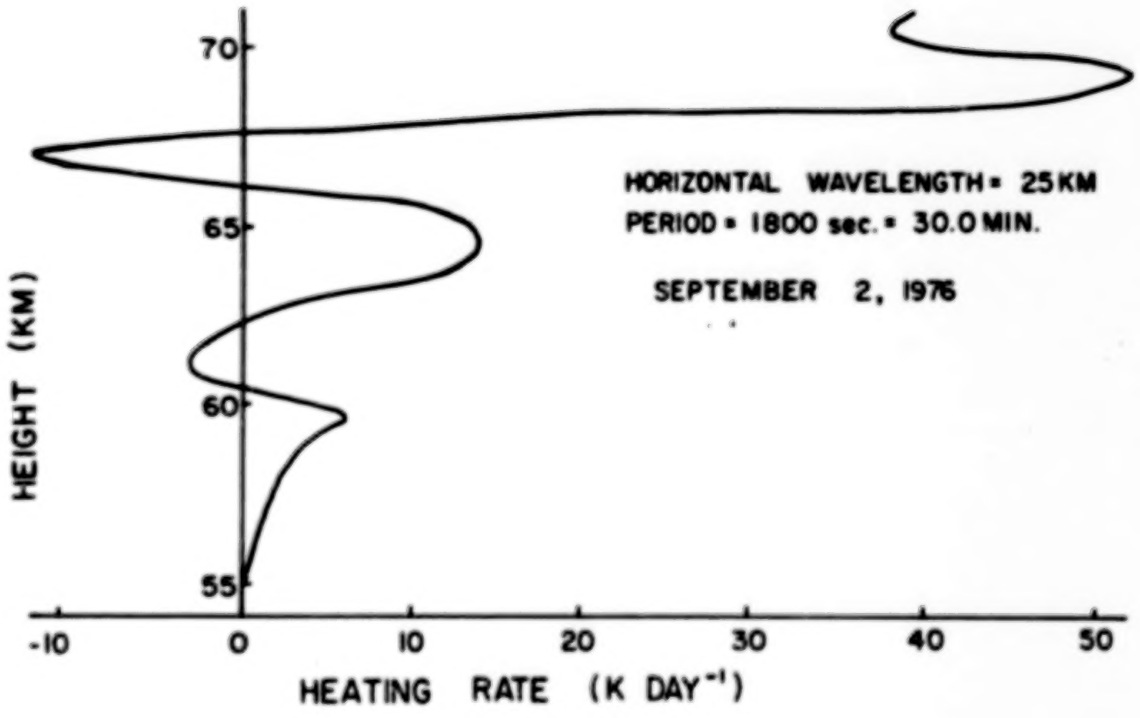

Figure 15. Heating rates as a function of height, September 2, 1976.

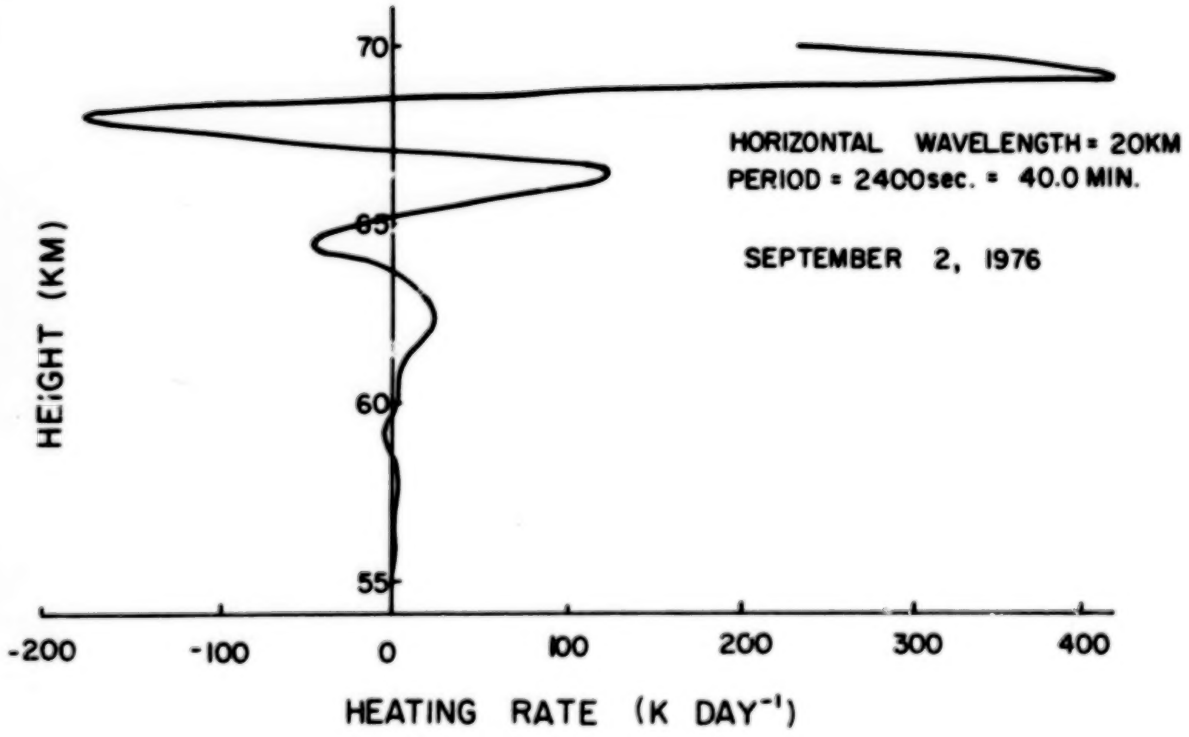

Figure 16. Heating rates as a function of height, September 2, 1976.

CHAPTER VII. CONCLUSIONS

The purpose of this thesis was to determine whether heating produced by gravity waves at an altitude of 60-70 kilometers could be responsible for the rapid heating observed in rocket measurements. The results seem to indicate that gravity waves are the probable mechanism producing that heating, despite all the assumptions and approximations made.

A review of the assumptions is presented here.

1. The assumptions of the parcel method (listed in Chapter II)
2. The assumption that all the parcel's kinetic energy becomes associated with the parcel's vertical velocity at the EL
3. The assumptions associated with ray-tracing theory
   a. the background atmosphere is
      incompressible
      isothermal
      isentropic
      hydrostatic
      non-rotating
   b. waves and atmosphere must obey the WKB approximation, i.e., variables are slowly varying over a wavelength
4. The assumptions associated with the set of equations used to find the vertical gravity wave structure in Chapter V
   a. again, the WKB approximation
   b. nonlinear terms are small and may be ignored
   c. a wave form for $\tilde{w}$ and $\tilde{u}$ with real wavenumber and frequency
   d. compressible and non-rotating atmosphere
   e. no friction
5. The assumption that the amount of frictional dissipation is calculated using waves that traveled to mesospheric heights with no friction
6. The assumption that the friction term may be estimated by means of an eddy viscosity coefficient

7. The assumption that all the energy dissipated by friction goes into heating the local medium

From this list of assumptions, the limitations of this particular approach of calculating the heating rates become readily apparent. The large amplitudes of u' and w' evident particularly above 70 kilometers in Figures 8 and 9 make it unreasonable to assume linear solutions as in this model. Therefore, rates obtained above 70 kilometers are not considered valid. Even below 70 kilometers the amplitudes in some cases are large enough to demand that nonlinear terms be accounted for. The large amplitudes and the complications introduced by the nonlinearities may be reduced if a friction term is included in the equations of motion used to determine the detailed structure of the gravity waves. This was not done in this study because of the great difficulty of solving such a set of equations.

Most of these assumptions (particularly the last three) will lead to overestimation of the heating rates. Therefore, large rates will be expected but if some correction factor could be applied to the rates accounting for all the overestimations, heating similar to that observed would very likely be the result. The large rates shown in the figures then tend to substantiate the claim that the heating is indeed a product of gravity wave interaction with the atmosphere.

The waves also produce cooling in certain regions. This is easily explained. Dissipation by friction is a process in which perturbations in a system become smoothed and flattened out. This is done not only by depositing energy in regions (heating) but also by removing energy from other regions (cooling). Note that even with cooling there is always net heating in the 60-70 kilometer range.

Another interesting feature in the plots of the heating rates is revealed through the shape of the plots and not the actual values. In all the plots, the calculated heating begins to take on significant values at the level at which the heating was actually observed. It seems as if heating by gravity waves only takes on significance above approximately 60 kilometers which may be why the heating is only noticeable above that level.

If gravity waves generated by convection in thunderstorms do produce heating of the magnitude observed consistently (other processes in the atmosphere may mask the effect at times), then in regions of the earth where thunderstorms and intense convection occur frequently, such as the tropics, the mesosphere may have slightly higher temperatures. This remains to be determined.

This study has produced no evidence that gravity waves are <u>not</u> the mechanism responsible for the observed heating. Any mechanism capable of coupling two regions of the atmosphere is potentially important so it is recommended that now a more detailed study should be made involving fewer simplifying assumptions and using equations for the gravity wave structure that include a friction term.

Since intense convection occurs somewhere on the earth practically every minute of every day, upper atmospheric measurements made at other sites should eventually coincide with the passage of a squall line. Such occurrences should be watched for. Similar warmings in other locations will validate the Wallops Island data and provide more cases for study. A special program involving a series of rocket launchings before, during and after intense convective events would also

help to better determine the existence, extent and intensity of the heating.

In Chapter III, the importance of the background wind in determining the paths and range of gravity wave groups was discussed. Given that importance, a study of the variability of stratospheric and mesospheric winds would be of use. A look at the sensitivity of wave propagation to wind and temperature values would also be of interest.

All of these suggestions will lead to a much-needed understanding of how events occurring in distant and seemingly distinct regions of the atmosphere are related. It is hoped that this understanding will serve as another step towards understanding the behavior of the atmosphere as a whole.

REFERENCES

Beer, Tom, 1974: Atmospheric Waves. John Wiley and Sons, 300 pp.

Bretherton, F. P., 1966: The propagation of groups of internal gravity waves in a shear flow. Quart. J. Roy. Meteor. Soc., 92, 466-480.

Bruce, G. H., D. W. Peaceman, H. E. Rachford, Jr. and J. D. Rice, 1953: Calculations of unsteady-state gas flow through porous media. Trans. Am. Inst. Min. Metall. Engnrs., 198, 79-92.

Chapman, S., and R. S. Lindzen, 1970: Atmospheric Tides, Thermal and Gravitational. D. Reidel Publishing Co., Dordrecht, Holland, 200 pp.

Cunnold, D., F. Alyea, N. Phillips and R. Prinn, 1975: A three-dimensional dynamical-chemical model of atmospheric ozone. J. Atmos. Sci., 32, 170-194.

Gossard, E. E., 1962: Vertical flux of energy into the lower ionosphere from internal gravity waves generated in the troposphere. J. Geophys. Res., 67, 745-757.

Gossard, E. E., and W. H. Hooke, 1975: Waves in the Atmosphere. Elsevier Scientific Publishing Co., 456 pp.

Harris, K. K., G. W. Sharp and W. C. Knudsen, 1969: Gravity waves observed by ionospheric temperature measurements in the F region. J. Geophys. Res., 74, 197-204.

Hess, Seymour L., 1959: Introduction to Theoretical Meteorology. Holt, Rinehart and Winston, 362 pp.

Hines, C. O., 1960: Internal atmospheric gravity waves at ionospheric heights. Can. J. Phys., 38, 1441-1481.

_____, 1963: The upper atmosphere in motion. Quart. J. Roy. Meteor. Soc., 89, 1-42.

_____, 1965: Dynamical heating of the upper atmosphere. J. Geophys. Res., 70, 177-183.

Hooke, William H., 1977: Rossby-planetary waves, tides, and gravity waves in the upper atmosphere. The Upper Atmosphere and Magnetosphere, National Academy of Sciences, Washington, D.C., 130-140.

Iribarne, J. V., and W. L. Godson, 1973: Atmospheric Thermodynamics. D. Reidel Publishing Co., Dordrecht, Holland, 222 pp.

Midgley, J. E., and H. B. Liemohn, 1966: Gravity waves in a realistic atmosphere. J. Geophys. Res., 71, 3729-3748.

Pierce, A. D., and S. C. Coroniti, 1966: A mechanism for the generation of acoustic-gravity waves during thunderstorm generation. Nature, 210, 1209-1210.

Riddle, Douglas F., 1970: Calculus and Analytic Geometry. Wadsworth Publishing Co., Inc., 731 pp.

Stull, Roland B., 1976: Internal gravity waves generated by penetrative convection. J. Atmos. Sci., 33, 1279-1286.

Townsend, A. A., 1965: Excitation of internal waves by a turbulent boundary layer. J. Fluid Mech., 22, 241-252.

_____, 1966: Internal waves produced by a convective layer. J. Fluid Mech., 24, 307-319.

_____, 1968: Excitation of internal waves in a stably-stratified atmosphere with considerable wind shear. J. Fluid Mech., 32, 145-171.

U. S. Standard Atmosphere, 1962: U. S. Government Printing Office, Washington, D.C.

Whitaker, W. A., 1963: Heating of the solar corona by gravity waves. Astrophys. J., 137, 914-930.

Zimmerman, S. P., and A. C. Faire, 1970: Internal gravity waves observed in mesospheric temperature measurements. AFCRL-70-0383, Aeronomy Laboratory Project 6690, Air Force Cambridge Research Laboratories, U. S. Air Force, 13 pp.

1. Report No.	2. Government Accession No.	3. Recipient's Catalog No.
NASA CR-3132		

4. Title and Subtitle	5. Report Date
MESOSPHERIC HEATING DUE TO INTENSE TROPOSPHERIC CONVECTION	April 1979
	6. Performing Organization Code

7. Author(s)	8. Performing Organization Report No.
Lauren Ludlum Taylor	
	10. Work Unit No.

9. Performing Organization Name and Address	11. Contract or Grant No.
The Pennsylvania State University The Graduate School Department of Meteorology University Park, PA 16802	NAS6-2818
	13. Type of Report and Period Covered
12. Sponsoring Agency Name and Address	Final
National Aeronautics and Space Administration Wallops Flight Center Wallops Island, VA 23337	14. Sponsoring Agency Code

15. Supplementary Notes

16. Abstract

A series of rocket measurements made twice daily by NASA at Wallops Island, Va., over the period of August 15 - September 10, 1976, revealed a rapid heating of the mesosphere on the order of 10 K on days when thunderstorms or squall lines were in the area. This heating is explained as the result of frictional dissipation of vertically propagating internal gravity waves generated by intense tropospheric convection.

An analysis of the tropospheric soundings for those days yields an estimate of the energy available to excite gravity waves. However, not all gravity waves will reach the level of heating. Some will be absorbed at critical levels or reflected back towards the surface. Ray-tracking theory is used to determine the spectrum of gravity wave groups that actually reach mesospheric heights. This knowledge is used in an equation developed by Stull (1976) describing the spectral energy density of a penetrative convective element to calculate the fraction of the total energy initially available to excite those waves that do reach the level of heating.

This value, converted into a vertical velocity, is used as the lower boundary condition for a multilayer model used to determine the detailed structure of the vertically propagating waves. The model does not include the effects of friction. The amount of frictional dissipation produced by the waves is calculated from the solutions of the frictionless model by use of a vertically varying eddy viscosity coefficient. The heating produced by the dissipation is then calculated from the thermodynamic equation.

Heating rates calculated from waves propagating with no friction are expected to be over-estimates of the actual heating by at least a factor of two. With this in mind, the rates obtained suggest that vertically propagating gravity waves are capable of producing the observed heating.

17. Key Words (Suggested by Author(s))	18. Distribution Statement
Meteorology Sounding Rockets Mesosphere Atmospheric Heating Gravity Waves Atmospheric Temperature Free Convection Convection Ray Tracing	Unclassified - Unlimited STAR Category 47

19. Security Classif. (of this report)	20. Security Classif. (of this page)	21. No. of Pages	22. Price*
Unclassified	Unclassified	61	

*For sale by the National Technical Information Service, Springfield, Virginia 22151

NASA-Langley, 1979

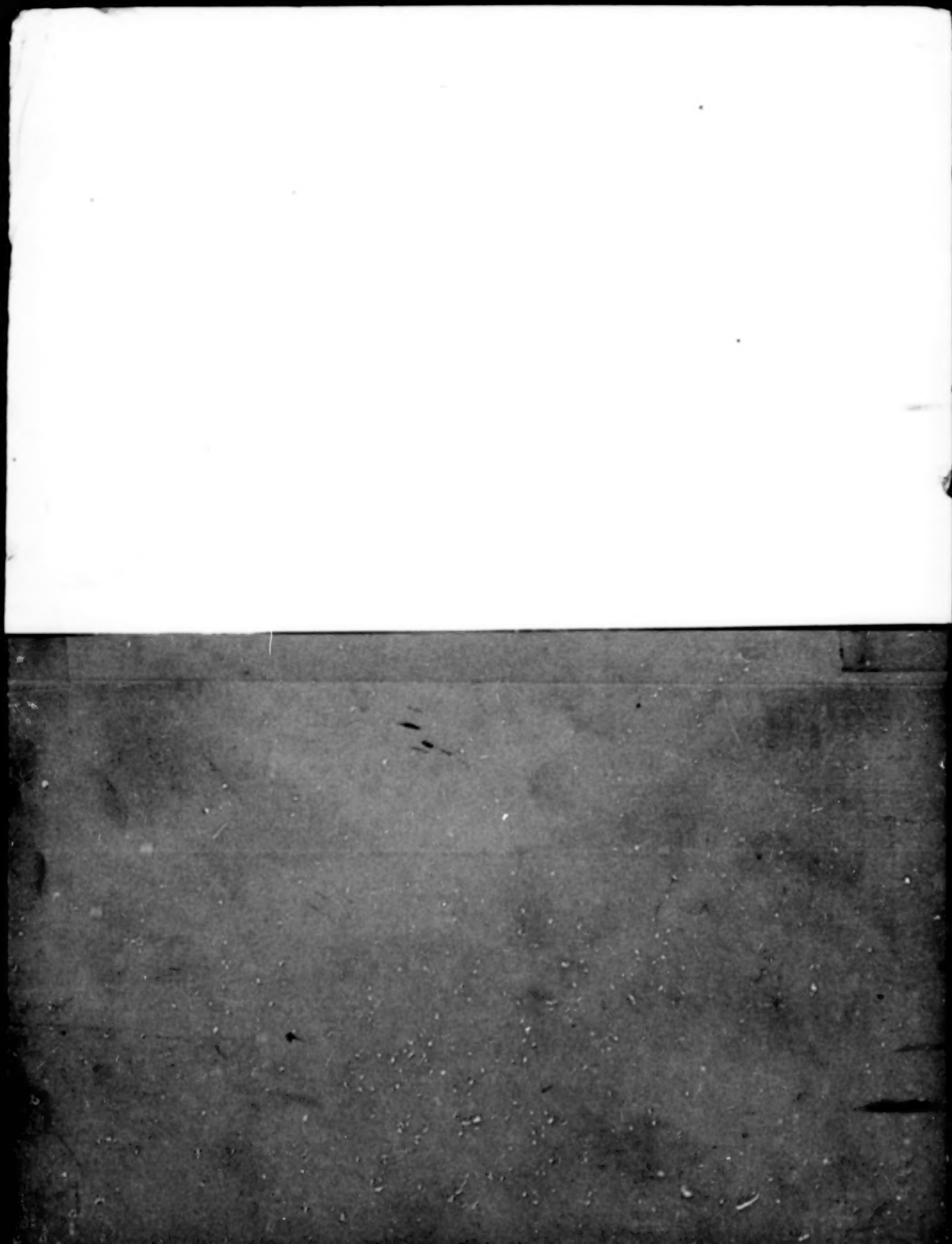

END

June 22, 1981